JACS
JOURNAL OF THE AMERICAN CHEMICAL SOCIETY
pubs.acs.org/JACS

Article

Photochemical and Thermal Concerted 1,3-Sigmatropic Rearrangements of a π-Extended Methylenecyclopropane

Shunsuke Konrai, Ma-aya Takano, Manabu Abe,* Hiroyasu Sato, Ryohei Kishi,* Takashi Kubo,* and Tomohiko Nishiuchi*

Cite This: J. Am. Chem. Soc. 2025, 147, 38700−38710

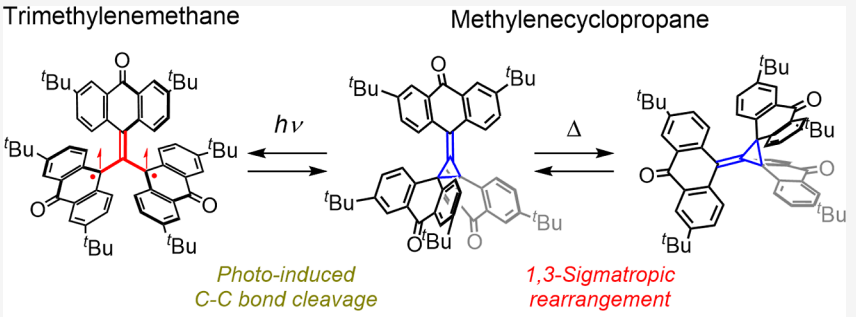

Spin-state control and dynamic C-C bond fluxionality by external stimuli

ABSTRACT: The reversible interconversion between methylenecyclopropane (MCP) and trimethylenemethane (TMM) has been extensively studied, yet precise control over their spin states remains challenging. Here, we designed and synthesized a propeller-shaped π-extended MCP derivative and its corresponding TMM derivative with anthroxyl moieties. The MCP derivative was isolated as a stable compound, and upon photoirradiation, it generated the triplet-state TMM derivative, which reverted to the MCP derivative without decomposition. In contrast, thermal excitation induced a unique carbon−carbon bond fluxionality within the MCP core via a concerted 1,3-sigmatropic rearrangement rather than a stepwise diradical pathway. These findings demonstrate that external stimuli such as light and heat enable spin-state control and dynamic bond fluxionality, providing new insights into organic stimuli-responsive materials.

INTRODUCTION

The elucidation of the properties and reactivity control of highly reactive chemical species such as cations, anions, and radicals has recently attracted increasing attention, as it serves as a foundation for the synthesis of compounds with complex electronic states[1−5] and the development of novel skeletal transformation/construction reactions.[6−8] Trimethylenemethane (TMM) is one of the well-studied highly reactive species, which exists in a triplet ground state (ΔE_{ST} = +16.1 kcal mol^{-1}, Figure 1a).[9−13] Photolysis of 4-methylene-Δ1-pyrazoline or 3-methylenecyclobutene can generate TMM only in low-temperature matrix at −196 °C, but at −150 °C, TMM rapidly cyclizes within minutes to form a stable closed-shell species, methylenecyclopropane (MCP). MCP undergoes a retrocyclization upon heating, regenerating TMM, but it is also known to undergo carbon−carbon bond exchange, forming a cyclopropane ring again at different carbon−carbon positions.[14−18] Two mechanisms have been proposed for this reaction: a concerted 1,3-sigmatropic rearrangement and a stepwise mechanism involving a twisted open-shell singlet diradical intermediate (Figure 1b). Previous studies have revealed that the carbon−carbon (C−C) bond exchange proceeds via the stepwise mechanism involving the open-shell singlet diradical intermediate.[6,19−21] Although TMM generated by the elimination of CO or N_2 initially shows triplet character before cyclizing to MCP, upon thermal retrocyclization of MCP, the open-shell singlet diradical intermediate is formed. This suggests that the triplet or singlet state of TMM can be controlled depending on the method of generation. If it becomes possible to repeatedly generate stable singlet and triplet states in TMM derivatives by applying external stimuli such as light, heat, or mechanical force to the MCP framework, this could open the potential for applications in stimuli-responsive magnetic materials based on organic compounds.[22−27] Furthermore, the C−C bond rearrangement in MCP is an attractive function to create a unique dynamical

Received: August 6, 2025
Revised: September 28, 2025
Accepted: September 29, 2025
Published: October 10, 2025

https://doi.org/10.1021/jacs.5c13563
J. Am. Chem. Soc. 2025, 147, 38700−38710

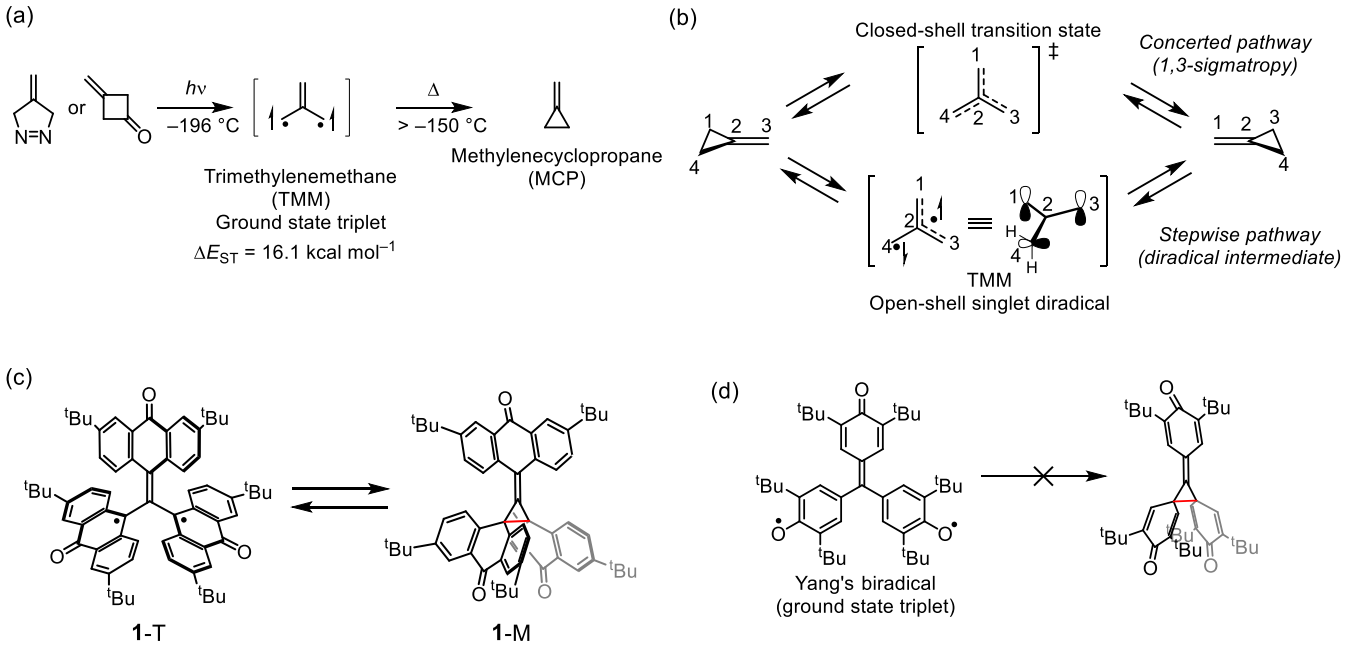

Figure 1. (a) Photoirradiation method for the generation of trimethylenemethane (TMM) with ground-state triplet and thermal ring closure to methylenecyclopropane (MCP). (b) Thermal C−C bond rearrangement of MCP and two rearrangement mechanisms, concerted and stepwise pathways. (c) π-extended TMM derivative **1**-T and corresponding MCP derivative **1**-M. (d) Typical π-extended TMM of Yang's biradical.

aromatic π-system as well as to understand the nature of the C−C bond.[28−34]

In this study, we designed a propeller-shaped π-extended TMM derivative, **1**-T, where the TMM framework is extended into three bulky anthroxyl skeletons (Figure 1c). A π-extended TMM derivative with three phenoxyl groups, known as Yang's biradical, is a relatively stable TMM derivative in a triplet ground state,[35] but due to spin delocalization onto the oxygen atoms, it does not form MCP, a hallmark of TMM reactivity (Figure 1d). On the other hand, in the anthroxyl framework, the spin density on the oxygen atom is reduced compared to the phenoxyl framework, and it is known that the spin density becomes dominant on the carbons at the 9-positions.[36] Therefore, the formation of MCP skeleton **1**-M, which was not observed in Yang's biradical, is expected. By applying external stimuli to **1**-M, we hypothesized that **1**-T could be regenerated as a stable species because the propeller structure composed of three bulky anthroxyl groups kinetically and thermodynamically stabilizes the reactive center of the TMM unit.[37] In this article, we report the synthesis and fundamental properties of the π-extended MCP derivative **1**-M and TMM derivative **1**-T. We successfully isolated **1**-M as a stable compound. By photoirradiation, a stable triplet species of TMM derivative **1**-T was generated and reverted to **1**-M without decomposition. On the contrary, upon heating **1**-M in solution, a C−C bond exchange rapidly occurred, but unlike existing MCP derivatives, it proceeded without passing through an open-shell singlet diradical intermediate, instead undergoing a 1,3-sigmatropic rearrangement. These findings demonstrate that external stimuli, such as heat and light, induce C−C bond fluxion on the MCP core, affording a dual potential energy surface derived from the closed-shell singlet and triplet states in the ground state.

RESULTS AND DISCUSSION

Synthesis and X-ray Structural Analysis. The synthetic procedure for **1**-M and **1**-T is shown in Figure 2a. Integration of three bulky aromatic units in the central TMM backbone was achieved by employing Negishi coupling conditions between **2** and the corresponding anthryl zinc reagent, yielding **3** in 64%. Demethylation of the methoxy groups of **3** using tribromoborane afforded **4**. Interestingly, compound **4** was partially oxidized by air in solution, resulting in one of the target compounds **1**-M being obtained as a mixture. Thus, the crude material of **4** was directly used for the generation of **1**-M and **1**-T by using potassium ferricyanide as an oxidant.

Fortunately, the stability of **1**-M is high enough to handle under ambient conditions, and a single crystal suitable for the measurement of X-ray crystallography was obtained, and structural analysis of **1**-M was unambiguously performed as shown in Figures 2b,c and S1. As aforementioned, the spin density of the anthroxyl radical localizes at the 9-position of carbon, and two anthroxyl radicals strongly interact in a face-to-face manner, affording a MCP core composed of an anthrone dimer. The central anthroquinomethyl unit is slightly bent toward the MCP core (θ_3 = 12°). In the X-ray crystallographic analysis, the recrystallization solvent of hexafluorobenzene was found to lie above the anthroquinomethyl unit; however, the bending is not induced by this solvent molecule but rather arises from steric hindrance of the anthrone dimer, as also reproduced by the optimized structure obtained from quantum chemical calculations (Figure S2). Regarding the C−C bond lengths in the MCP core, C1−C2 and C2−C3 (C2−C3′) are usual lengths at 1.341(3) Å for a double bond and at 1.467(2) Å for a single bond, respectively. On the other hand, due to bulky anthroxyl units integrated face-to-face, the bond length at C3−C3′ is 1.680(3) Å, which is a long C−C bond and seems readily dissociating to afford the **1**-T. These bond lengths are reflected on the bond angles in MCP that are θ_1 = 69.9° and θ_2 = 55.1°. To evaluate the

https://doi.org/10.1021/jacs.5c13563
J. Am. Chem. Soc. 2025, 147, 38700−38710

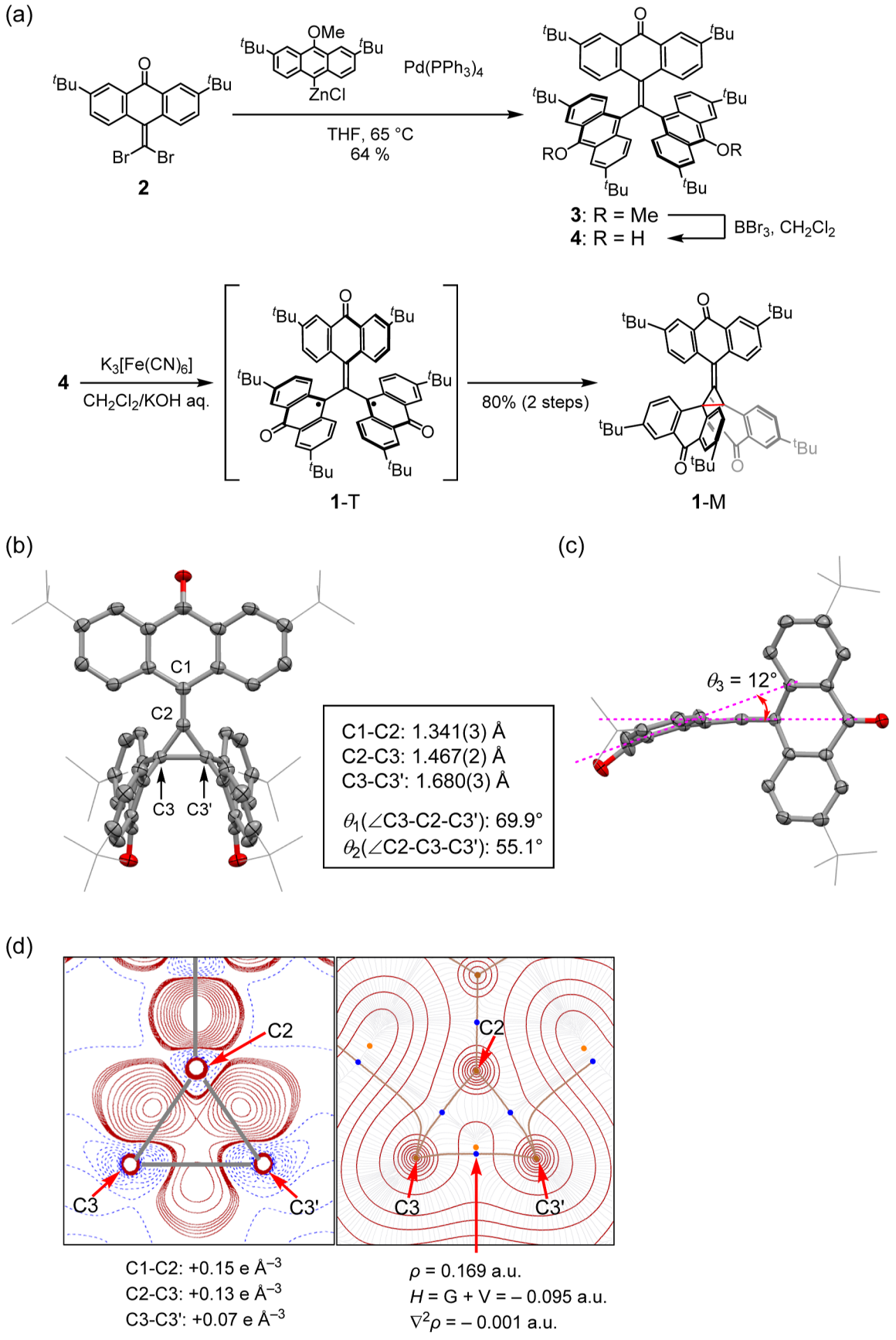

Figure 2. (a) Synthetic route to **1**-M and **1**-T. (b) Front view of the molecular structure of **1**-M. Structural parameters such as C−C bond lengths and bond angles of the central TMM unit are summarized. (c) Side view of **1**-M. Hydrogens are omitted, and *tert*-butyl groups are represented by wireframes for clarity. Thermal ellipsoids at 50% probability. (d) Electron density distribution (EDD) analysis map (left) and atom in molecules

https://doi.org/10.1021/jacs.5c13563
J. Am. Chem. Soc. 2025, 147, 38700−38710

Figure 2. continued

analysis map (right) focused on the MCP core (C2−C3−C3′ plane) of **1**-M. The red lines in EDD represent positive contours from 0.01 to 0.05 e Å^{-3} in steps of 0.01 e Å^{-3}. The blue dashed lines in EDD represent negative contours from −0.05 to −0.50 e Å^{-3} in steps of −0.05 e Å^{-3}.

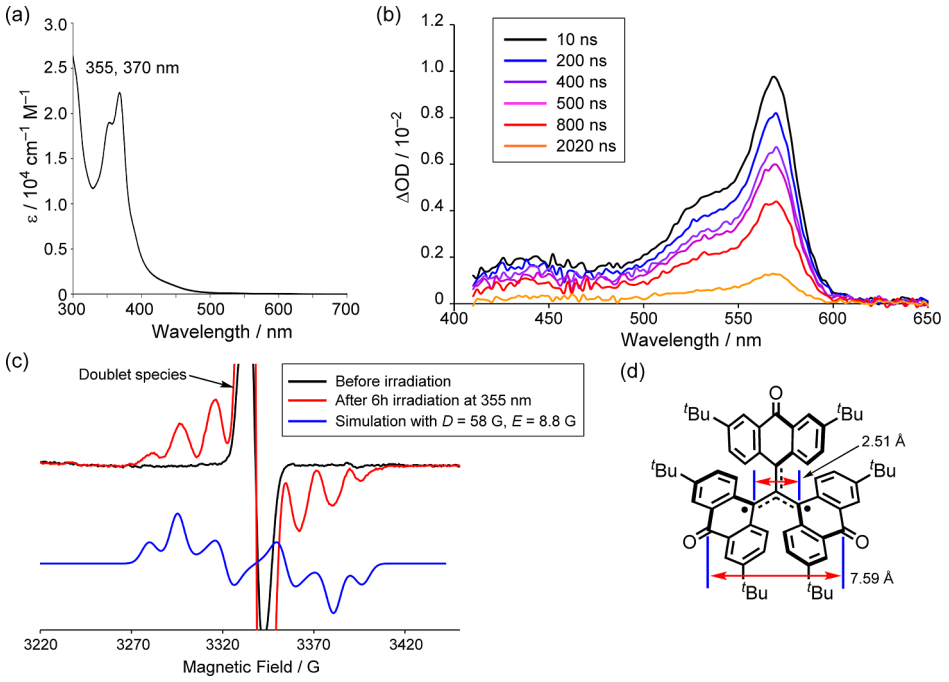

Figure 3. (a) UV−vis spectrum of **1**-M in benzene. (b) Transient absorption spectrum of **1**-M in benzene. (c) ESR spectrum of **1**-M before irradiation (black) and after irradiation at 85 K (red) in 2-methyltetrahydrofuran (10 mM) and simulated spectra (blue). (d) Carbon−carbon distances of the MCP core and carbonyl carbons between two anthroxyl units in **1**-T.

hybridization state of C3 (C3′), the π-orbital axis vector (POAV) analysis method, which involves a structural deformation analysis of an sp^2 carbon atom from planarity, was employed (Figure S1d).[38] The POAV pyramidalization angle (θ_p) of C3 was found to be 4.86°, suggesting a slight deviation from perfect sp^2 hybridization. This hybridization state is fully consistent with the NBO analysis (B3LYP-D3/6-311+G**), thereby indicating that the orbitals involved in the bonding interaction between C3 and C3′ possess significant 2p character (p % = 89%) with a small contribution of 2s character (s % = 11%). To gain deeper insight into the electronic interaction between C3 and C3′, electron density distribution (EDD) analysis was performed to visualize the distribution of valence electrons in the crystalline state, and the static model deformation density map of **1**-M on the plane of the MCP core is shown in Figure 2d. A concentration of electron density apparently exists in between C3 and C3′ about +0.07 e Å^{-3}, which is relatively lower than the other C−C bonds between C1−C2 (+0.15 e Å^{-3}) and C2−C3 (+0.13 e Å^{-3}). Atom in molecules (AIM) analysis[39] based on the theoretical electron density, which was determined by a B3LYP-D3/6-311+G** calculation using the X-ray structure, also showed a bond critical point (BCP) between C3 and C3′. The BCP exhibits the electron density ρ = 0.169 au, the total electron energy density H = −0.095 au, and the Laplacian of the electron density $\nabla^2\rho$ = −0.001 au, which satisfies the criteria of a covalent bond in the AIM analysis. To further evaluate the structures of **1**-M and **1**-T, quantum chemical calculations were performed (Figure S2). The calculated structure of **1**-M is in good agreement with the results of X-ray analysis. Regarding the spin state of **1**-T, both open-shell singlet diradical and triplet states are considered, and the calculations indicate that the energy of the triplet state is lower than that of the open-shell singlet diradical state. The energetically most stable state is **1**-M, but the energy difference between **1**-M and **1**-T (triplet) is estimated to be only 1.86 kcal mol^{-1} ((U)B3LYP-D3/6-311+G**). Therefore, external stimuli-induced structural changing (spin-state changing) between **1**-M and **1**-T was expected.

Photostimulated Generation of 1-T. The external stimuli-induced structural change between **1**-M and **1**-T was performed by using the flash photolysis technique in solution. The steady-state UV−vis spectrum of **1**-M shows a broad weak band from 400 to 500 nm and intense peaks at 370 and 355 nm (Figure 3a). On the other hand, the transient absorption spectroscopy of **1**-M revealed that a transient species with absorption at 570 and 535 nm was observed (Figure 3b). The result of TD-DFT calculations of **1**-T is highly consistent with this transient absorption (Table S1 and Figures S3 and S4). ESR measurement of **1**-M at 85 K with photoirradiation (355 nm) exhibited zero-field splitting with |D| = 5.80 mT and |E| = 0.88 mT, which is characteristic for a triplet species (Figure 3c). The average spin−spin distance was estimated from the |D| value to be 7.88 Å by a point-dipole approximation. Comparison with the optimized structure obtained from quantum chemical calculations shows that this distance is much closer to the carbonyl carbon−carbon separation between the anthroxyl units (7.59 Å) than to the central TMM core carbon−carbon distance (2.51 Å) (Figure 3d). Thus, unpaired electrons of **1**-T delocalize onto anthroxyl

https://doi.org/10.1021/jacs.5c13563
J. Am. Chem. Soc. 2025, 147, 38700−38710

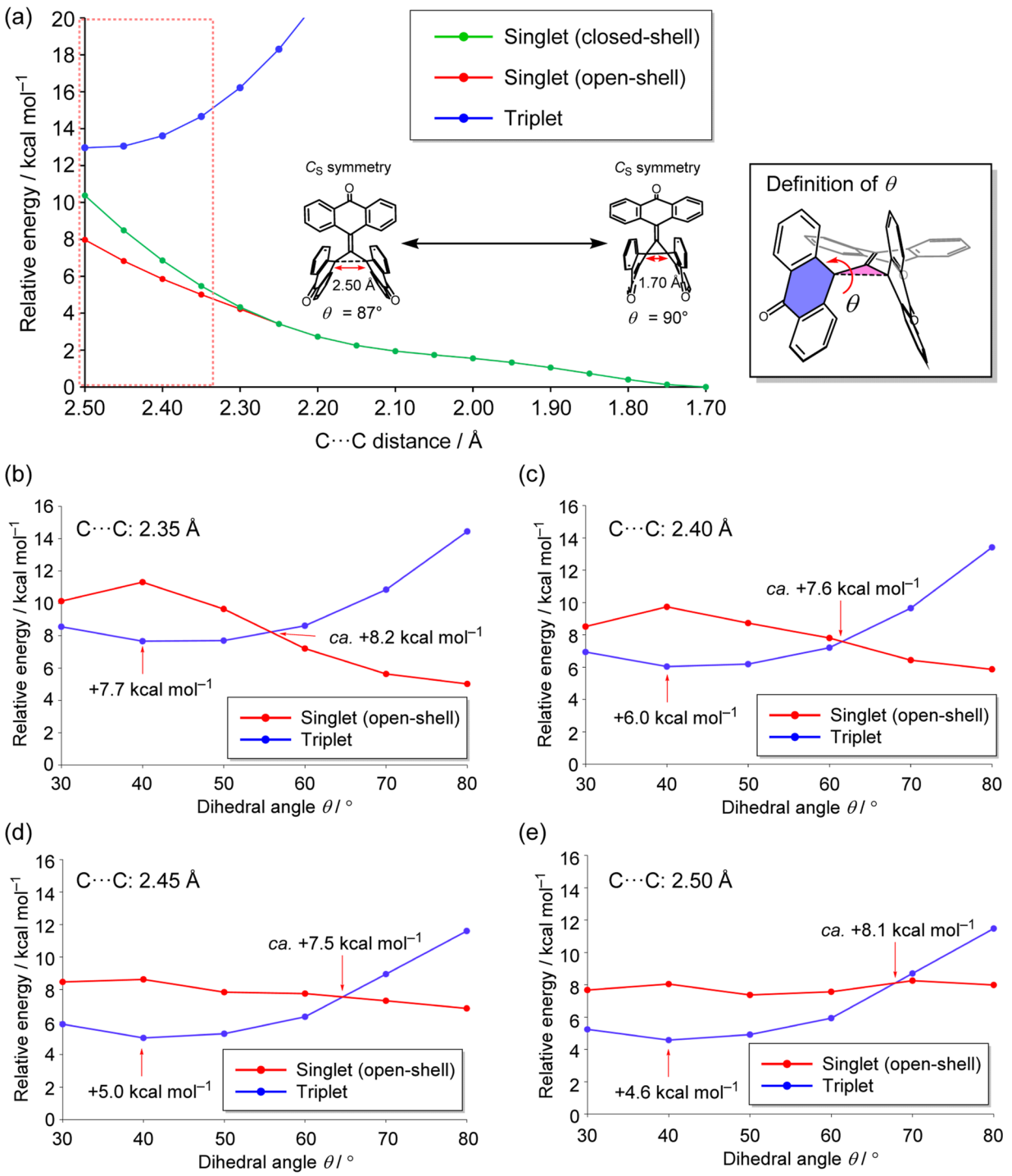

Figure 4. (a) Relative energy potential curve of **1**-M for the C−C distance. (b)−(e) Relative energy potential curves of the singlet (open-shell) structures derived from **1**-M and the corresponding triplet-state structures as a function of the dihedral angle θ of the anthroxyl unit, where θ is defined as the angle between the plane of the three carbon atoms of the cyclopropane core (shown in pink) and the mean plane of the central six-membered ring of the anthrone unit (shown in purple) ((U)B3LYP-D3/6−31G*).

units, which is confirmed by quantum chemical calculations (Figure S2c). Such delocalization of spin density onto the carbonyl oxygen atoms is expected to facilitate spin inversion, which can rationalize why the photogenerated triplet state **1**-T readily reverts to the closed-shell **1**-M despite the spin-forbidden nature of direct recombination. After the transient absorption measurement, no spectral changing of UV−vis of **1**-M was confirmed, indicating that the generated **1**-T thermally reverts to **1**-M without decomposition (Figure S7). The half-life (τ) of **1**-T was determined to be 1.04 μs under an argon atmosphere. Interestingly, the τ under an oxygen atmosphere is 0.93 μs, which is almost no quenching by oxygen, probably because the steric hindrance of the large π-blade of three anthroxyl units effectively suppresses the quenching of the triplet state from oxygen (Figure S8). By changing the measurement temperature of the decay profile, the thermodynamic parameters $\Delta H_{(T \rightarrow M)}^{\ddagger}$ and $\Delta S_{(T \rightarrow M)}^{\ddagger}$ for the reversion from **1**-T to **1**-M were determined to be 3.68 kcal

https://doi.org/10.1021/jacs.5c13563
J. Am. Chem. Soc. 2025, 147, 38700−38710

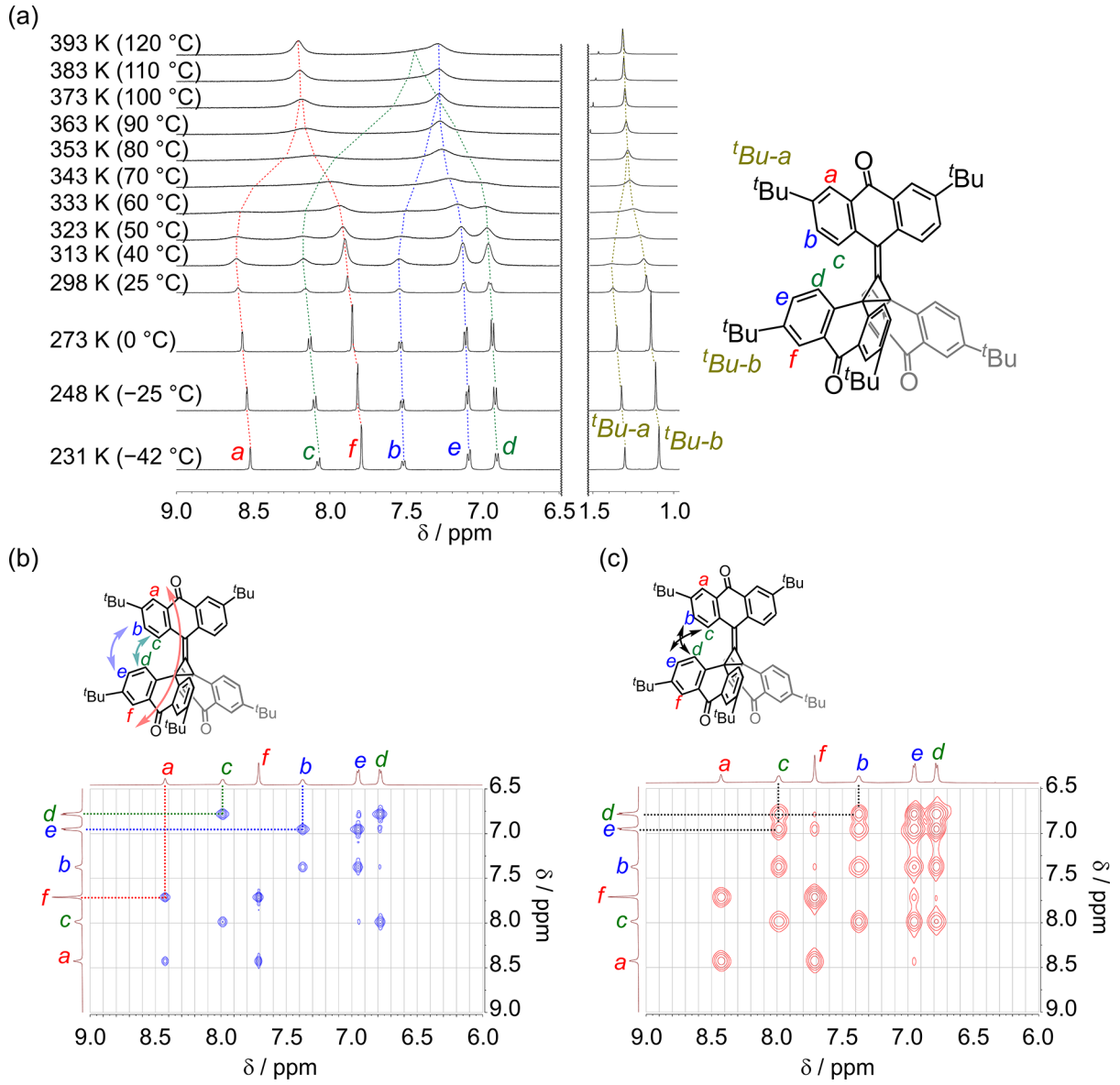

Figure 5. (a) VT ^{1}H NMR spectra of **1**-M measured in 1,1,2,2-tetrachloroethane-d_2. (b) ^{1}H−^{1}H EXSY spectrum of **1**-M in the range of 9−6 ppm, measured in 1,1,2,2-tetrachloroethane-d_2 at 298 K (mixing time = 200 ms). Cross-correlations between protons *a* and *f*, *b* and *e*, and *c* and *d* are depicted with red, blue, and green lines, respectively. (c) ^{1}H−^{1}H TOCSY spectrum of **1**-M in the range of 9−6 ppm, measured in 1,1,2,2-tetrachloroethane-d_2 at 298 K (mixing time = 30 ms). Cross-correlations between protons *b* and *d* and *c* and *e* are depicted with black lines.

mol^{-1} and −18.1 cal mol^{-1} K^{-1}, respectively (Figure S9), corresponding to $\Delta G_{(T\rightarrow M,\ 298\ K)}^{\ddagger}$ = 9.07 kcal mol^{-1}. The negative entropy term is due to the ring-closing reaction from TMM to MCP. The activation energy E_a for this reversion is to be 4.31 kcal mol^{-1}, which is consistent with that of nonsubstituted TMM to MCP (2.0 to 5.0 kcal mol^{-1}).[12]

To further investigate the reversion mechanism from **1**-T to **1**-M, quantum chemical calculations (B3LYP-D3/6−31G*) were performed to construct potential energy curves as a function of the C−C distance and the dihedral angle (θ), where θ is defined as the angle between the plane of the three carbon atoms of the cyclopropane core and the mean plane of the central six-membered ring of the anthrone unit, starting from the **1**-M geometry with a C−C distance of 1.7 Å. When the C−C distance is less than 2.30 Å, the closed-shell singlet is the most stable form. At distances greater than 2.30 Å, however, the system begins to exhibit singlet diradical character (Figure 4a). Nevertheless, the energy of the triplet state remains higher than that of the singlet states due to strong antiparallel spin−spin interactions in the face-to-face arrangement of the anthroxyl units. Therefore, using the optimized structures of the open-shell singlet and triplet states at C−C distances exceeding 2.30 Å, we systematically varied the dihedral angle between the two anthroxyl units (Figure 4b−e). As the dihedral angle decreases, the energy of the open-shell singlet gradually increases, whereas that of the triplet state gradually decreases, ultimately leading to the formation of a propeller-shaped, stable triplet structure (C−C: 2.50 Å and θ = 40°), which lies +4.6 kcal mol^{-1} above **1**-M (C−C: 1.70 Å and θ = 90°). The activation energy for the **1**-T to **1**-M conversion, estimated from the crossing point of the potential energy curves of triplet and singlet (open-shell) states (+7.5−8.2 kcal mol^{-1}), is calculated to be 2.9−3.6 kcal mol^{-1}, which is in good

https://doi.org/10.1021/jacs.5c13563
J. Am. Chem. Soc. 2025, 147, 38700−38710

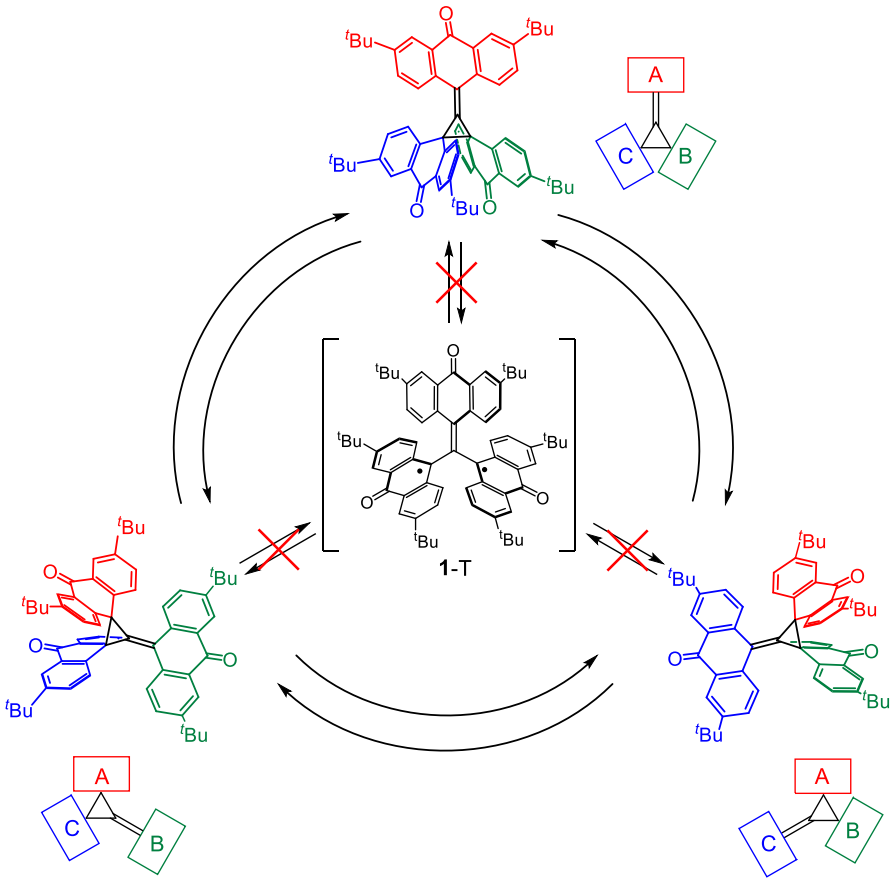

Figure 6. Schematic illustration of the fluxional C−C bond of **1**-M without forming the triplet intermediate of **1**-T.

agreement with the experimental results (E_a = 4.31 kcal mol^{-1}).

NMR Study on the 1,3-Sigmatropic C−C Bond Fluxion of the MCP Core. The thermally accessible triplet state of singlet diradicals has been extensively studied. For compound **1**-M, structural conversion to **1**-T via thermal excitation in solution was anticipated. To evaluate the generation of **1**-T, variable-temperature (VT) ^{1}H NMR measurements of **1**-M were conducted. At room temperature (298 K), the ^{1}H NMR signals of **1**-M appeared slightly broadened, but they became sharper upon cooling (Figure 5a). This behavior initially seems to imply an increase in the population of the thermally excited triplet state at elevated temperatures, associated with the opening of the MCP core to form a TMM core; however, as clarified in the following analyses, this possibility was excluded. Upon heating, the ^{1}H NMR signals of **1**-M broaden further between 313 and 343 K compared to those at 298 K. Interestingly, however, the broadened peaks become sharper again at 393 K. In addition, several proton signals (*a* and *f*, *b* and *e*, *c* and *d*, ^{t}Bu-*a* and ^{t}Bu-*b*) gradually coalesce into a highly symmetric pattern. This signal behavior suggests that the broadening is not due to thermal generation of the triplet state **1**-T. This conclusion is further supported by VT-ESR measurements, which show no indication of thermally generated **1**-T but only show a signal originating from the doublet impurity of **1**-IM (Figure S10). Notably, **1**-IM can be obtained as a minor byproduct when recrystallization of **1**-M is carried out under air, where partial oxidation of **1**-M leads to the incorporation of **1**-IM crystals. Thus, dynamic structural rearrangement within the MCP core could be considered as another possible origin of the signal broadening.

To gain further insight into the dynamics of **1**-M, ^{1}H−^{1}H exchange spectroscopy (EXSY) was performed to examine the anthroxyl ring exchange (Figure 5b). Notably, even at room temperature (298 K), cross-peaks are observed between *a* and *f*, between *b* and *e*, and between *c* and *d*, indicating mutual exchange of proton positions. Furthermore, total correlation spectroscopy (TOCSY) measurements show cross-peaks between *b* and *d* and between *c* and e, protons that do not belong to the same anthroxyl ring, indicating exchange between rings (Figure 5c). These experimental results provide clear evidence that **1**-M undergoes continuous dissociation and reformation of the C−C bond in solution due to fluxional motion within the MCP core without forming the triplet intermediate of **1**-T (Figure 6). The C−C bond exchange rate (k_{ex}) between 298 and 393 K was determined by line-shape analysis of the VT ^{1}H NMR spectra (Figure S11). The values of k_{ex} were found to be 9 s^{-1} at 298 K and 12,000 s^{-1} at 393 K. Thermodynamic activation parameters $\Delta H_{(C-C)}^{\ddagger}$ and $\Delta S_{(C-C)}^{\ddagger}$ were obtained from an Eyring plot based on these rates (Figure S12), yielding $\Delta H_{(C-C)}^{\ddagger}$ = 16.8 kcal mol^{-1} and $\Delta S_{(C-C)}^{\ddagger}$ = 2.11 cal mol^{-1} K^{-1}, which correspond to $\Delta G_{(C-C,\ 298\ K)}^{\ddagger}$ = 16.2 kcal mol^{-1}. The positive entropy term is consistent with a ring-opening process in the MCP core. Notably, the activation enthalpy is significantly lower than that of previously reported MCP derivatives.[6,17,18] However, compared to the calculated and experimental energy differences between **1**-T and **1**-M (from photochemical studies), these values are relatively high, suggesting that the C−C bond

https://doi.org/10.1021/jacs.5c13563
J. Am. Chem. Soc. 2025, 147, 38700−38710

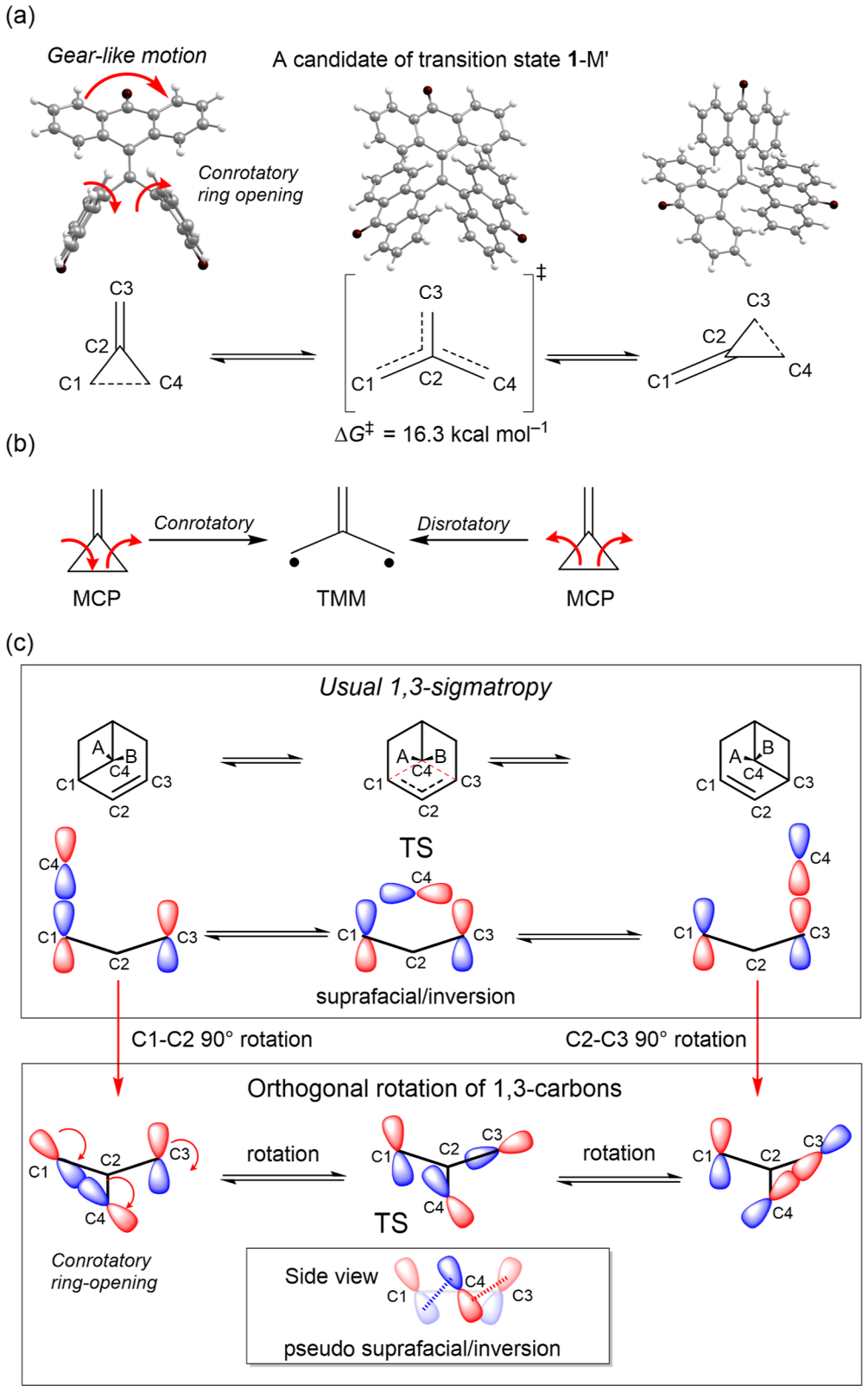

Figure 7. (a) Molecular structure of a candidate transition state **1**-M′ for the 1,3-sigmatropic shift together with its Gibbs free energy barrier (293 K) and structural changes in the central TMM core during the 1,3-sigmatropic shift. Calculations were performed at the B3LYP/6-311+G* level of theory. (b) General schematic illustration of the two possible ring-opening pathways of an MCP core leading to a TMM framework (not specific to the present system). (c) Molecular orbital description for a usual 1,3-sigmatropic carbon shift (up)[41] and the case of C−C bond fluxion of **1**-M (down). Reproduced from ref 41. Copyright [1967] American Chemical Society.

fluxion in **1**-M does not proceed through **1**-T as an intermediate.

To understand the C−C bond fluxionality in the MCP core, we conducted computational studies. Since the experimental

https://doi.org/10.1021/jacs.5c13563
J. Am. Chem. Soc. 2025, 147, 38700−38710

results suggest that the fluxional process does not proceed via the triplet intermediate **1**-T, we explored an alternative pathway involving **1**-M′, a closed-shell singlet species and a candidate for the transition state, using spin-restricted DFT calculations (Figure 7a and Figure S13). Although the intrinsic reaction coordinate (IRC) calculation could not be completed due to the presence of a shallow plateau on the potential energy surface near the first-order saddle point (Figure S14−S15), the apparent Gibbs free energy barrier ($\Delta G_{cal}^{\ddagger}$) of **1**-M′ was calculated to be 16.3 kcal mol^{-1} at 298.15 K, in good agreement with the experimental value ($\Delta G_{exp}^{\ddagger}$ = 16.2 kcal mol^{-1} at 298 K). This result suggests that the fluxional process may proceed via a concerted mechanism, consistent with a 1,3-sigmatropic rearrangement. Two possible mechanisms have been proposed for C−C bond rearrangements in MCP derivatives: stepwise and concerted. Experimental and computational studies have previously supported only the stepwise pathway involving a twisted TMM intermediate in a singlet diradical state. To clarify why **1**-M follows a concerted 1,3-sigmatropic pathway, frontier molecular orbital analysis was employed. The ring-opening of the MCP core can, in theory, occur via a conrotatory or disrotatory motion (Figure 7b). In **1**-M, however, the bulky face-to-face anthroxyl units with their extended π-systems impose significant steric constraints, allowing only a conrotatory ring-opening pathway. This conrotatory rotation of the two anthroxyl units induces a counter-rotation of the third, resembling a gear-like motion. At the transition state, the p-orbital on the migrating carbon C4 undergoes a 1,3-shift of the propenyl π-system from C1 to C3 with steric inversion. Based on the selection rules for carbon-based 1,3-sigmatropic rearrangement proposed by Woodward and Hoffmann,[40] the symmetrically allowed pathways are that the p-orbital of migrating carbon interacts with the allylic π-system as a suprafacial interaction with steric inversion and an antrafacial interaction with steric retention. Because of the antrafacial pathway being geometrically unfeasible, only the suprafacial pathway with steric inversion of the migrating carbon has been observed (Figure 7c).[41,42] Although the bonding interaction mode of the 1,3-shift in **1**-M′ seemed to be antarafacial, the propenyl π-orbital between C1−C2 and C2−C3 in TMM has an unusual orthogonal twist system. In addition, during the 1,3-shift, the propenyl π-orbital continuously rotates. Thus, the bonding interaction mode in **1**-M′ can be classified as suprafacial. This interaction satisfies the selection rules for a symmetry-allowed 1,3-sigmatropic rearrangement of a carbon atom. Consequently, the generation of triplet **1**-T via spin inversion seems to be suppressed, as the p-orbitals in the MCP core appear to remain in bonding interaction throughout the rearrangement, as suggested by the HOMO and HOMO−1 of **1**-M′ (Figure S13b). Thus, the thermal C−C bond fluxion of **1**-M proceeds not through the lower-energy **1**-T intermediate (accessible only via photo-irradiation) but rather via a higher-energy closed-shell singlet pathway through **1**-M′, probably due to a weak spin−orbit coupling at the minimum energy crossing point between singlet and triplet energy surfaces.[43−46] While this mechanistic proposal is supported by both experimental data and DFT calculations, and the chosen computational level is consistent with previous studies on related diradicaloid hydrocarbons and has been shown to reproduce experimental S−T gaps reliably,[34,47,48] further refinement through higher-level computational methods, including potential energy surface mapping and nonadiabatic dynamics simulations, will provide deeper insights into the full reaction pathway and the interplay between spin states in this unique fluxional system.

CONCLUSION

In this article, we designed the π-extended MCP **1**-M and TMM **1**-T, which contain an appended anthroxyl moiety, and the MCP **1**-M was isolated as a stable form. Photoirradiation of **1**-M readily produces **1**-T, which was unambiguously characterized by a transient measurement technique. The generated **1**-T reverts to **1**-M by pathing potential energy surfaces from triplet to singlet in the ground state without decomposition. On the other hand, **1**-M shows continuous C−C bond dissociation and formation, and, during the process, the existence of a closed-shell transition state **1**-M′ was proposed experimentally and computationally. Based on the Woodward−Hoffmann rule, the C−C bond fluxion of **1**-M occurs by a 1,3-sigmatropic mechanism due to the structural restriction of large anthroxyl π-blades, which was first discovered in the history of TMM/MCP chemistry. These findings demonstrate that external stimuli, such as heat and light, induce dynamic structural changes with the C−C bond fluxionality, enabling spin-state control of either an open-shell triplet or a closed-shell singlet in the ground state.

ASSOCIATED CONTENT

Supporting Information

The Supporting Information is available free of charge at https://pubs.acs.org/doi/10.1021/jacs.5c13563.

Full synthetic, crystallographic, and computational details as well as spectroscopic data for new compounds (PDF)

Accession Codes

Deposition Numbers 2428897 and 2486260 contain the supplementary crystallographic data for this paper. These data can be obtained free of charge via the joint Cambridge Crystallographic Data Centre (CCDC) and Fachinformations-zentrum Karlsruhe AccessStructuresservice.

AUTHOR INFORMATION

Corresponding Authors

Manabu Abe − *Department of Chemistry, Graduate School of Advanced Science and Engineering, Hiroshima University, Higashi-Hiroshima, Hiroshima 739-8526, Japan;* orcid.org/0000-0002-2013-4394; Email: mabe@hiroshima-u.ac.jp

Ryohei Kishi − *Department of Materials Engineering Science, Graduate School of Engineering Science, The University of Osaka, Osaka 560-8531, Japan; Innovative Catalysis Science Division, Institute for Open and Transdisciplinary Research Initiatives, (ICS-OTRI), The University of Osaka, Osaka 565-0871, Japan; Research Center for Solar Energy Chemistry (RCSEC) and Center for Quantum Information and Quantum Biology (QIQB), The University of Osaka, Osaka 560-8531, Japan;* orcid.org/0000-0002-6005-7629; Email: kishi.ryohei.es@osaka-u.ac.jp

Takashi Kubo − *Department of Chemistry, Graduate School of Science, The University of Osaka, Osaka 560-0043, Japan; Innovative Catalysis Science Division, Institute for Open and Transdisciplinary Research Initiatives, (ICS-OTRI), The University of Osaka, Osaka 565-0871, Japan;* orcid.org/0000-0001-6809-7396; Email: kubo@chem.sci.osaka-u.ac.jp

https://doi.org/10.1021/jacs.5c13563
J. Am. Chem. Soc. 2025, 147, 38700−38710

Tomohiko Nishiuchi − *Department of Chemistry, Graduate School of Science, The University of Osaka, Osaka 560-0043, Japan; Innovative Catalysis Science Division, Institute for Open and Transdisciplinary Research Initiatives, (ICS-OTRI), The University of Osaka, Osaka 565-0871, Japan;* orcid.org/0000-0002-2113-0731; Email: nishiuchit13@chem.sci.osaka-u.ac.jp

Authors

Shunsuke Konrai − *Department of Chemistry, Graduate School of Science, The University of Osaka, Osaka 560-0043, Japan*

Ma-aya Takano − *Department of Chemistry, Graduate School of Advanced Science and Engineering, Hiroshima University, Higashi-Hiroshima, Hiroshima 739-8526, Japan*

Hiroyasu Sato − *Rigaku Corporation, Tokyo 196-8666, Japan*

Complete contact information is available at: https://pubs.acs.org/10.1021/jacs.5c13563

Author Contributions

All authors have given approval to the final version of the manuscript.

Notes

The authors declare no competing financial interest.

■ ACKNOWLEDGMENTS

This study was supported by JSPS KAKENHI Grant Numbers JP24K01454 (T. N.), JP20H05865 (T. K.), JP24H00459 (T. K.), JP25K22260 (M. A.), JP22H04974 (R. K.), and JP22H02050 (R. K.), by a research grant from Takahashi Industrial and Economic Research Foundation (T. N.), and in part by JST CREST JPMJCR20R4 (M. A.). Quantum chemical calculations were performed at the Research Center for Computational Science, Okazaki, Japan (Projects: 24-IMS-C214, 25-IMS-C291, and 25-IMS-C004). This work was the result of using research equipment shared in the MEXT Project for promoting public utilization of advanced research infrastructure (Program for supporting construction of core facilities, Grant Number JPMXS0441200024).

■ REFERENCES

(1) Olah, G. A. Carbocations and Electrophilic Reactions. *Angew. Chem., Int. Ed. Engl.* **1973**, *12*, 173−254.
(2) Shoji, Y.; Tanaka, N.; Mikami, K.; Uchiyama, M.; Fukushima, T. A two-coordinate boron cation featuring C−B$^+$−C bonding. *Nat. Chem.* **2014**, *6*, 498−503.
(3) Abe, M. Diradicals. *Chem. Rev.* **2013**, *113*, 7011−7088.
(4) Kato, K.; Osuka, A. Platforms for Stable Carbon-Centered Radicals. *Angew. Chem., Int. Ed.* **2019**, *58*, 8978−8986.
(5) Kubo, T. Syntheses and Properties of Open-Shell π-Conjugated Molecules. *Bull. Chem. Soc. Jpn.* **2021**, *94*, 2235−2244.
(6) Nakamura, E.; Yamago, S. Thermal Reactions of Dipolar Trimethylenemethane Species. *Acc. Chem. Res.* **2002**, *35*, 867−877.
(7) Kamitani, M.; Nakayasu, B.; Fujimoto, H.; Yasui, K.; Kodama, T.; Tobisu, M. Single−carbon atom transfer to α,β-unsaturated amides from N-heterocyclic carbenes. *Science* **2023**, *379*, 484−488.
(8) Shoji, Y.; Tanaka, N.; Muranaka, S.; Shigeno, N.; Sugiyama, H.; Takenouchi, K.; Hajjaj, F.; Fukushima, T. Boron-mediated sequential alkyne insertion and C−C coupling reactions affording extended π-conjugated molecules. *Nat. Commun.* **2016**, *7*, 12704.
(9) Dowd, P. Trimethylenemethane. *Acc. Chem. Res.* **1972**, *5*, 242−248.
(10) Baseman, R. J.; Pratt, D. W.; Chow, M.; Dowd, P. T. Trimethylenemethane. Experimental demonstration that the triplet state is the ground state. *J. Am. Chem. Soc.* **1976**, *98*, 5726−5727.
(11) Platz, M. S.; McBride, J. M.; Little, R. D.; Harrison, J. J.; Shaw, A.; Potter, S. E.; Berson, J. A. Triplet ground states of trimethylenemethanes. *J. Am. Chem. Soc.* **1976**, *98*, 5725−5726.
(12) Dowd, P.; Chow, M. T. Trimethylenemethane. Activation energy for the ring closure of a 1,3 diradical. *J. Am. Chem. Soc.* **1977**, *99*, 6438−6440.
(13) Wenthold, P. G.; Hu, J.; Squires, R. R.; Lineberger, W. C. Photoelectron Spectroscopy of the Trimethylenemethane Negative Ion. The Singlet−Triplet Splitting of Trimethylenemethane. *J. Am. Chem. Soc.* **1996**, *118*, 475−476.
(14) Kon, G. A. R.; Nanji, H. R. 380. The structure of the glutaconic acids and esters. Part VII. Derivatives of 3-methylcyclopropene-1 : 2-dicarboxylic acid. *J. Chem. Soc.* **1932**, 2557−2568.
(15) Chesick, J. P. Kinetics of the Thermal Interconversion of 2-Methylmethylenecyclopropane and Ethylidenecyclopropane. *J. Am. Chem. Soc.* **1963**, *85*, 2720−2723.
(16) Gilbert, J. C.; Butler, J. R. Degeneracy in the Methylenecyclopropane Rearrangement. *J. Am. Chem. Soc.* **1970**, *92*, 2168−2169.
(17) Kirmse, W.; Murawski, H.-R. Thermal Rearrangement of 1-Alkoxy-2-methylenecyclopropanes. *J. Chem. Soc. Chem. Commun.* **1977**, *51*, 122−123.
(18) LeFevre, G. N.; Crawford, R. J. Kinetics of Some Methylenecyclopropane Rearrangements. *J. Org. Chem.* **1986**, *51*, 747−749.
(19) Gajewski, J. J. Hydrocarbon Degenerate Thermal Rearrangements. II. Stereochemistry of the Methylenecyclopropane Self-Interconversion. *J. Am. Chem. Soc.* **1968**, *90*, 7178−7179.
(20) Abe, M.; Adam, W. Electronic substituent effects on the EPR-spectral D parameter of trimethylenemethane (TMM) triplet diradicals compared with localized cyclopentane-1,3-diyls. *J. Chem. Soc., Perkin Trans.* **1998**, *2*, 1063−1068.
(21) Creary, X. Super Radical Stabilizers. *Acc. Chem. Res.* **2006**, *39*, 761−771.
(22) Sato, O.; Tao, J.; Zhang, Y.-Z. Control of Magnetic Properties through External Stimuli. *Angew. Chem., Int. Ed.* **2007**, *46*, 2152−2187.
(23) Nishiuchi, T.; Ito, R.; Stratmann, E.; Kubo, T. Switchable conformational isomerization of an overcrowded tristricyclic aromatic ene. *J. Org. Chem.* **2020**, *85*, 179−186.
(24) Ishigaki, Y.; Hashimoto, T.; Sugawara, K.; Suzuki, S.; Suzuki, T. Switching of Redox Properties Triggered by a Thermal Equilibriumbetween Closed-Shell Folded and Open-Shell Twisted Species. *Angew. Chem., Int. Ed.* **2020**, *59*, 6581−6584.
(25) Suzuki, S.; Yamaguchi, D.; Uchida, Y.; Naota, T. Hysteretic Control of Near-infrared Transparency Using a Liquescent Radical Cation. *Angew. Chem., Int. Ed.* **2021**, *60*, 8284−8288.
(26) Nishiuchi, T.; Aibara, S.; Sato, H.; Kubo, T. Synthesis of π-Extended Thiele's and Chichibabin's Hydrocarbons and Effect of the π-Congestion on Conformations and Electronic States. *J. Am. Chem. Soc.* **2022**, *144*, 7479−7488.
(27) Ishigaki, Y.; Harimoto, Y.; Shimajiri, T.; Suzuki, T. Carbon-based Biradicals: Structural and Magnetic Switching. *Chem. Rev.* **2023**, *123*, 13952−13965.
(28) Abe, M.; Adam, W.; Heidenfelder, T.; Nau, W. M.; Zhang, X. Intramolecular and Intermolecular Reactivity of Localized Singlet Diradicals: The Exceedingly Long-Lived 2,2-Diethoxy-1,3-diphenylcyclopentane-1,3-diyl. *J. Am. Chem. Soc.* **2000**, *122*, 2019−2026.
(29) Schreiner, P. R.; Chernish, L. V.; Gunchenko, P. A.; Tikhonchuk, E. Y.; Hausmann, H.; Serafin, M.; Schlecht, S.; Dahl, J. E. P.; Carlson, R. M. K.; Fokin, A. A. Overcoming Lability of Extremely Long Alkane Carbon−Carbon Bonds through Dispersion Forces. *Nature* **2011**, *477*, 308−311.
(30) Rösel, S.; Balestrieri, C.; Schreiner, P. R. Sizing the Role ofLondon Dispersion in the Dissociation of All-meta tert-Butyl Hexaphenylethane. *Chem. Sci.* **2017**, *8*, 405−410.
(31) Ishigaki, Y.; Shimajiri, T.; Takeda, T.; Katoono, R.; Suzuki, T. Longest C−C Single Bond among Neutral Hydrocarbons with a Bond Length beyond 1.8 Å. *Chem.* **2018**, *4*, 795−806.

(32) Li, J.; Pang, R.; Li, Z.; Lai, G.; Xiao, X.-Q.; Müller, T. Exceptionally Long C−C Single Bonds in Diamino-o-Carborane asInduced by Negative Hyperconjugation. *Angew. Chem., Int. Ed.* **2019**, *58*, 1397−1401.
(33) Shimajiri, T.; Kawaguchi, S.; Suzuki, T.; Ishigaki, Y. Direct evidence for a carbon-carbon one-electron σ-bond. *Nature* **2024**, *634*, 347−351.
(34) Kubo, T.; Suga, Y.; Hashizume, D.; Suzuki, H.; Miyamoto, T.; Okamoto, H.; Kishi, R.; Nakano, M. Long Carbon−Carbon Bonding beyond 2 Å in Tris(9-fluorenylidene)methane. *J. Am. Chem. Soc.* **2021**, *143*, 14360−14366.
(35) Yang, N. C.; Castro, A. J. SYNTHESIS OF A STABLE BIRADICAL. *J. Am. Chem. Soc.* **1960**, *82*, 6208.
(36) Hirao, Y.; Saito, T.; Kurata, H.; Kubo, T. Isolation of a Hydrogen-Bonded Complex Based on the Anthranol/Anthroxyl Pair: Formation of a Hydrogen-Atom Self-Exchange System. *Angew. Chem., Int. Ed.* **2015**, *54*, 2402−2405.
(37) Nishiuchi, T.; Aibara, S.; Kubo, T. Synthesis and Properties of a Highly Congested Tri(9-anthryl)methyl Radical. *Angew. Chem., Int. Ed.* **2018**, *57*, 16516−16519.
(38) Haddon, R. C. Comment on the Relationship of the Pyramidalization Angle at a Conjugated Carbon Atom to the σ Bond Angles. *J. Phys. Chem. A* **2001**, *105*, 4164−4165.
(39) Bader, R. F. W. Atoms in Molecules. *Acc. Chem. Res.* **1985**, *18*, 9−15.
(40) Woodward, R. B.; Hoffmann, R. Selection Rules for Sigmatropic Reactions. *J. Am. Chem. Soc.* **1965**, *87*, 2511−2513.
(41) Berson, J. A.; Nelson, G. L. Inversion of Configuration in the Migrating Group of a Thermal 1,3-Sigmatropic Rearrangement. *J. Am. Chem. Soc.* **1967**, *89*, 5503−5504.
(42) Dietrich, K.; Musso, H. Notiz zur thermischen Valenzisomerisierung des Norpinens. *Chem. Ber.* **1974**, *107*, 731−734.
(43) Liu, S.; Srinivasan, S.; Tao, J.; Grady, M. C.; Soroush, M.; Rappe, A. M. Modeling Spin-Forbidden Monomer Self-Initiation Reactions in Spontaneous Free-Radical Polymerization of Acrylates and Methacrylates. *J. Phys. Chem. A* **2014**, *118*, 9310−9318.
(44) Fedorov, D. A.; Lykhin, A. O.; Varganov, S. A. Predicting Intersystem Crossing Rates with AIMS-DFT Molecular Dynamics. *J. Phys. Chem. A* **2018**, *122*, 3480−3488.
(45) Lykhin, A. O.; Kaliakin, D. S.; dePolo, G. E.; Kuzubov, A. A.; Varganov, S. A. Nonadiabatic Transition State Theory: Application to Intersystem Crossings in the Active Sites of Metal-Sulfur Proteins. *Int. J. Quantum Chem.* **2016**, *116*, 750−761.
(46) Tao, Y.; Pei, Z.; Bellonzi, N.; Mao, Y.; Zou, Z.; Liang, W.; Yang, Z.; Shao, Y. Constructing spin-adiabatic states for the modeling of spin-crossing reactions. I. A shared-orbital implementation. *Int. J. Quantum Chem.* **2020**, *120*, No. e26123.
(47) Rottschäfer, D.; Busch, J.; Neumann, B.; Stammler, H.-G.; van Gastel, M.; Kishi, R.; Nakano, M.; Ghadwal, R. S. Diradical Character Enhancement by Spacing: N-Heterocyclic Carbene Analogues of Müller's Hydrocarbon. *Chem.—Eur. J.* **2018**, *24*, 16537−16542.
(48) Dressler, J. J.; Barker, J. E.; Karas, L. J.; Hashimoto, H. E.; Kishi, R.; Zakharov, L. N.; MacMillan, S. N.; Gomez-Garcia, C. J.; Nakano, M.; Wu, J. I.; Haley, M. M. Late-Stage Modification of Electronic Properties of Antiaromatic and Diradicaloid Indeno[1,2-b]fluorene Analogues via Sulfur Oxidation. *J. Org. Chem.* **2020**, *85* (16), 10846−10857.

https://doi.org/10.1021/jacs.5c13563
J. Am. Chem. Soc. 2025, 147, 38700−38710